

Supramolecular Interaction of Primaquine with Native β -Cyclodextrin

M. Murugan^{1,3} · A. Anitha^{1,4} · K. Sivakumar⁵ ·
R. Rajamohan^{1,2}

Received: 19 September 2017 / Accepted: 27 March 2018 / Published online: 22 May 2018
© Springer Science+Business Media, LLC, part of Springer Nature 2018

Abstract The supramolecular host–guest inclusion complex of Primaquine (PQ) with the nano-hydrophobic cavity of beta-cyclodextrin (β -CD) was prepared by physical mixing, kneading and co-precipitation methods. The formation of an inclusion complex in PQ with β -CD in the solution phase has been confirmed by UV–visible and fluorescence spectroscopy. The stoichiometry of the inclusion complex is 1:1; the Primaquine molecule is deeply entrapped in the cavity of β -cyclodextrin, which was confirmed by analysis of spectral shifts and corresponding absorbance and fluorescence intensities. The Benesi–Hildebrand plot was used to calculate the binding constant of the inclusion complex of PQ with β -CD at room temperature. The Gibbs energy change of the inclusion complex process has been calculated. The pK_a and pK_a^* for the monocation and neutral equilibrium of PQ in aqueous and β -CD media are discussed. The thermal stability for the inclusion complex of PQ with β -CD has been analyzed using differential scanning calorimetry. The modification of the crystal structure to amorphous for the solid inclusion complex was confirmed by powder X-ray diffraction. The structure of the complex is proposed by docking studies using the Patch-Dock server. A cytotoxic analysis was also carried out for the pure PQ and its solid complex on the MDA MB 231 cell line and showed that the activity is good for both substances. The cytotoxicity neither improved nor decreased with the formation of the inclusion complex with β -CD.

Keywords Primaquine · β -CD · Acidity constants · DSC · Patch-Dock server · In-vitro anticancer activity

✉ R. Rajamohan
rajmohanau@gmail.com

¹ Research and Development Centre, Bharathiar University, Coimbatore, Tamil Nadu 641 046, India

² Department of Chemistry, SKP Engineering College, Tiruvannamalai, Tamil Nadu 606 611, India

³ Department of Chemistry, IFET College of Engineering, Villupuram, Tamil Nadu 605 108, India

⁴ Department of Chemistry, Government Arts College, Chidambaram, Tamil Nadu 608 102, India

⁵ Department of Chemistry, SCSVMV University, Kanchipuram, Tamil Nadu 631 561, India

1 Introduction

Primaquine is the only available drug for preventing relapse of malaria, and confusion surrounds its use [1]. Primaquine is used with other medications to prevent and treat malaria caused by mosquito bites in countries where malaria is common. Malaria parasites can enter the body through these mosquito bites, and then live in body tissues such as red blood cells or the liver. PQ has an unpleasant bitter taste, which is reduced by the addition of β -CD [2, 3].

In host–guest chemistry, an inclusion compound is a complex in which one chemical compound (the “host”) forms a cavity in which molecules of a second “guest” compound are located. The definition of inclusion compounds is very broad, extending to channels formed between molecules in a crystal lattice in which guest molecules can fit. If the spaces in the host lattice are enclosed on all sides so that the guest species is ‘trapped’ as in a cage, the compound is known as a clathrate. In molecular encapsulation a guest molecule is actually trapped inside another molecule [4].

Cyclodextrin molecules are cyclic oligosaccharides made up of six to twelve α -D-glucopyranose monomers, which are connected at the 1 and 4 carbon atoms. Cyclodextrins with six to eight α -D-glucopyranose units are denoted as α -, β - and γ -cyclodextrin respectively. Among these various types of cyclodextrins, α -cyclodextrin is not suitable for many drugs and γ -cyclodextrin is expensive. β -cyclodextrin is widely used because it is readily available, and its cavity size is suitable for a wide range of guest molecules. Addition of a hydrophobic guest to aqueous solutions of cyclodextrins leads to complexation in which no covalent bonds are broken or formed. In general, the special characteristic of cyclodextrins is the ability to form an inclusion complex with various organic molecules through host–guest interaction with the interior cavity that provides a hydrophobic environment to trap a polar molecule [5]. The interactions between host–guest molecules are formed by several weak forces, including van der Waals, hydrophobic, dipole–dipole and hydrogen bonding [6]. Several favorable changes in the physicochemical properties of the guest molecule are observed, including increased stability, dissolution rate, solubility, and bio-availability due to inclusion complex formation between the drug molecules with CDs [7–11]. The cyclodextrins are mostly used in pharmaceuticals [12], food [13], cosmetics [14], environment protection [15], bio-conversion [16], drug delivery [17], packing and the textile industry [18], amphiphiles [19], supramolecular polymers [20], bio-active materials [21], self-healing materials [22], nano-structures [23], or in the solubilization of hydrophobic monomers or RAFT agents [24, 25]. In this work we report the inclusion complex between PQ and β -CD in solution and in the solid state.

2 Materials and Methods

2.1 Reagents

β -Cyclodextrin (purity $\geq 99\%$) and Primaquine (PQ) (purity $\geq 99\%$) were obtained from the Sigma–Aldrich company. A stock solution of PQ ($1.8 \times 10^{-5} \text{ mol}\cdot\text{dm}^{-3}$) was prepared by using triply distilled water. The different concentration of stock solution of β -CD (0 to $12 \times 10^{-3} \text{ mol}\cdot\text{dm}^{-3}$) was prepared by using triply distilled water. All the experiments have been carried out using triply distilled water. The different concentration solutions were prepared before taking UV and fluorescence measurements.

3-(4,5-Dimethyl-thiazol-2-yl)-5-diphenyltetrazolium bromide (MTT), fetal bovine serum (FBS), phosphate buffered saline (PBS), Dulbecco's Modified Eagle's Medium (DMEM) and trypsin were obtained from Sigma–Aldrich Co., St. Louis, USA. EDTA, glucose and antibiotics were from Hi-Media Laboratories Ltd., Mumbai. Dimethylsulfoxide (DMSO) and propanol were from E-Merck Ltd., Mumbai, India.

2.2 Instruments

Absorption spectra are measured using a Shimadzu UV–2450PC spectrophotometer while fluorescence spectra of all the solution are recorded between 380 and 500 nm using a Perkin Elmer LS-45 fluorescence spectrophotometer. FT-IR spectra were recorded using a Thermo Nicolet iS5 FT-IR spectrophotometer as KBr pellets the range of 500–4000 cm^{-1} . Microscopic morphological structure measurements were implemented using an FEI Quanta FEG 200 scanning electron microscope (SEM). pH values of various solutions were measured using an ELICO LI-10T model pH-meter. Powder X-ray diffraction spectra were obtained using a D8 Advance X-ray instrument (Bruker, Germany) with 2.2 kW Cu anode, ceramic X-ray tube as the source and Lynx Eye (silicon strip detector technology) as the detector, Ni filter as the Beta filter and zero background sample holder, PMMA sample holder.

2.3 Molecular Docking Studies

The most probable structure of the complex was determined by a molecular docking study using the Patch-Dock server [26]. The three-dimensional structural data for β -CD and pure PQ was obtained from crystallographic databases. The PQ molecule was docked into the β -CD cavity using the Patch-Dock server by submitting the 3D coordinate data of PQ and β -CD molecules. Docking was performed with complex type configuration settings. The Patch-Dock server follows a geometry-based molecular docking algorithm to find the docking transformations with good molecular shape complementarity. Patch-Dock algorithm separates the Connolly dot surface representation [27, 28] of the molecules into concave, convex and flat patches. These divided complementary patches are matched in order to generate candidate transformations and evaluated by geometric fit and atomic desolvation energy scoring [29]. RMSD (root mean square deviation) clustering is applied to the docked solutions to select the non-redundant results and to discard redundant docking structures.

2.4 Semi-empirical Analysis

The optimized structure of PQ molecule in the ground state was calculated by the AM1 method.

2.5 Preparation of Inclusion Complex in Liquid Medium

The stock solution of PQ (1.8×10^{-5} mol·dm $^{-3}$ concentration) was prepared using distilled water and 0.3 mL of this solution was added to 5 mL volumetric flasks. It is made up to the mark to give the following concentrations of β -CD: 0.002, 0.004, 0.006, 0.008, 0.010 and 0.012 mol·dm $^{-3}$.

2.6 Preparation of Solid Inclusion Complexes of PQ with β -CD

The physical mixture (PM), kneading product (KM) and solid complexes were prepared by the physical method, kneading method and co-precipitation method, respectively, following literature procedures [30].

2.7 Determination of Acidity Constants

2.7.1 Ground state Acidity Constant (pK_a)

Absorption spectra of the acid and its conjugate base were sufficiently different that clear isosbestic points could be obtained. Two sets of wavelengths on either side of the isosbestic points were selected and absorbance at these wavelengths were measured. Calculations for different sets of λ values were also carried out separately. The concentration of each species at a different pH was calculated from Eqs. 1 and 2,

$$C_1 = \frac{A(\lambda_1)\varepsilon_2(\lambda_2) - A(\lambda_2)\varepsilon_2(\lambda_1)}{\varepsilon_2(\lambda_1)\varepsilon_2(\lambda_2) - \varepsilon_1(\lambda_2)\varepsilon_2(\lambda_1)} \quad (1)$$

$$C_2 = C_T - C_1 \quad (2)$$

where C_T is the total concentration of the compound in both forms and $\varepsilon_1(\lambda_1)$, $\varepsilon_1(\lambda_2)$, $\varepsilon_2(\lambda_1)$ and $\varepsilon_2(\lambda_2)$ are the molar extinction coefficients of species 1 and 2 at wavelengths λ_1 and λ_2 , respectively. The latter were determined from the absorbance at a $\text{pH} \geq \text{p}K_a \pm 2$ where only one species is present. The $\text{p}K_a$ for the equilibrium



where BH^+ is species 1 and B is species 2, was calculated by using the equation

$$\text{p}K_a = \text{pH} + \log_{10}(C_1/C_2) \quad (3)$$

2.7.2 Excited State Acidity Constant ($\text{p}K_a^*$)

The excited state acidity constants ($\text{p}K_a^*$) were obtained by the fluorimetric titration (FT) method [31, 32].

3 Results and Discussion

3.1 Interaction of PQ with β -CD in Liquid State

3.1.1 Absorption Spectral Characteristics of PQ in β -CD

From the absorption and emission spectra, we can determine the molecular recognition between host β -CD and guest PQ molecule in an aqueous solution. Thus, the absorption maximum (λ_{max}) increases with increasing concentration of β -CD, as shown in Fig. 1. The absorption band is observed for PQ in the absence of β -CD at 262.6 nm and shows slight blue shifts with significant changes in absorbance in solutions containing β -CD (Table 1). Moreover, the β -CD does not have any significant absorption or fluorescence intensities

Fig. 1 Absorption spectra of PQ ($1.8 \times 10^{-5} \text{ mol}\cdot\text{dm}^{-3}$) with increasing concentrations of β -CD at pH = 6.8 (1), 0; (2), 0.002; (3), 0.004; (4), 0.006; (5), 0.008, (6), 0.010 and (7), $0.012 \text{ mol}\cdot\text{dm}^{-3} \beta$ -CD

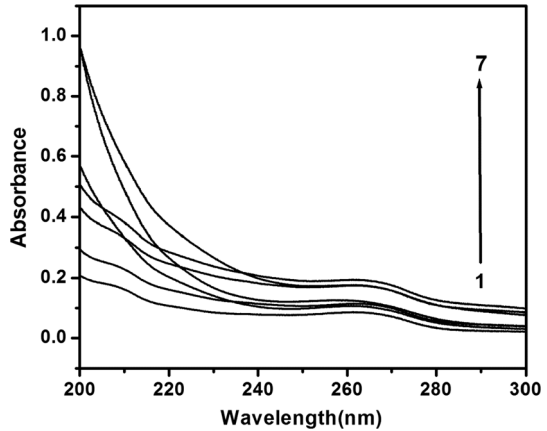


Table 1 The absorption and fluorescence spectral maxima of PQ in different concentrations of β -CD at pH = 6.8

S. no.	[β -CD] ($\text{mol}\cdot\text{dm}^{-3}$)	Absorption spectrum		Fluorescence spectrum			
		λ_{max} (nm)	Absorbance	λ_{flu} (nm)	Intensity	λ_{flu} (nm)	Intensity
1	0	262.6	0.08	–	–	375.0	89.19
2	0.002	262.5	0.10	358.1	265.12	372.0	283.76
3	0.004	261.5	0.11	358.5	409.83	372.0	438.91
4	0.006	261.5	0.12	357.1	613.54	372.0	664.06
5	0.008	260.8	0.17	357.1	618.11	371.0	649.52
6	0.010	260.4	0.17	357.1	619.01	371.0	667.53
7	0.012	258.8	0.19	361.5	711.22	371.0	809.52

[33] and could be ignored while analyzing the spectral changes for PQ. These observations clearly suggest the formation of an inclusion complex between guest and host molecules in the liquid state.

The following equilibrium (Eq. 4) is shown with the assumption of the 1:1 stoichiometric ratio of β -CD and PQ, is

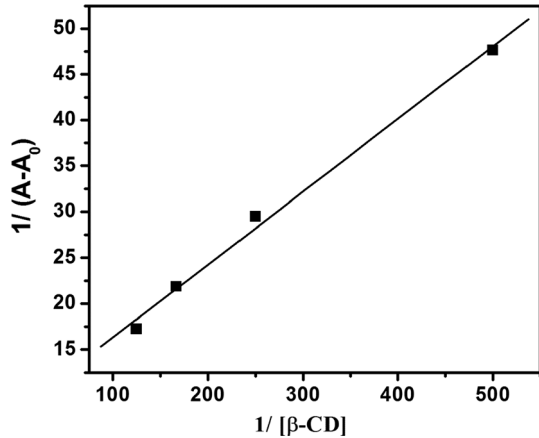


In order to determine the binding constant K and stoichiometry of PQ: β -CD complex, the Benesi–Hildebrand (BH) equation (Eq. 5) is used.

$$\frac{1}{A - A_0} = \frac{1}{\Delta\epsilon[\text{PQ}]_0} + \frac{1}{K\Delta\epsilon[\text{PQ}]_0[\beta\text{-CD}]_0} \quad (5)$$

A plot of $1/(A - A_0)$ against $1/[\beta\text{-CD}]$ gives a linear plot with a correlation coefficient $r^2 = 0.997$ (Fig. 2), which confirms the formation of a 1:1 stoichiometric complex. The binding constant K is calculated from the slope of the straight line and is found to be $114.48 \text{ dm}^3\cdot\text{mol}^{-1}$ at 303 K (Eq. 6).

Fig. 2 Benesi–Hildebrand absorption plot of $1/(A-A_0)$ against $1/[\beta\text{-CD}]$ for PQ



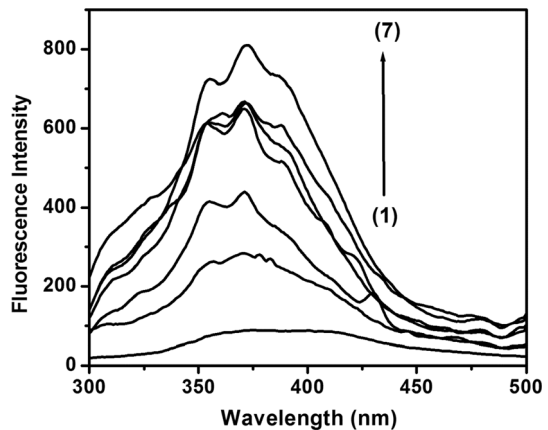
$$K = \frac{1}{\text{slope}(A - A_0)} \quad (6)$$

3.1.2 Emission Spectral Characteristic of PQ in $\beta\text{-CD}$

Figure 3 shows the fluorescence spectra of PQ without and with $\beta\text{-CD}$ up to the saturation level of complexation of PQ in $\beta\text{-CD}$ ($0.012 \text{ mol}\cdot\text{dm}^{-3}$). The fluorescence spectrum in aqueous solution gives a single maximum at 375.0 nm with 89.19 as fluorescence intensity. When $\beta\text{-CD}$ is added, the band at 375.0 nm is slightly blue shifted to 371.0 nm with an increase in the intensity of the fluorescence. Also, the addition of $\beta\text{-CD}$ causes the appearance of a new maximum at 358.1 nm in $0.002 \text{ mol}\cdot\text{dm}^{-3}$ $\beta\text{-CD}$. The fluorescence intensities for both maxima increase with increasing concentration of $\beta\text{-CD}$.

In order to confirm the dual maxima for PQ with $\beta\text{-CD}$, the fluorescence excitation spectra of PQ in $12 \times 10^{-3} \text{ mol}\cdot\text{dm}^{-3}$ $\beta\text{-CD}$ are recorded with different emission wavelengths. The excitation spectra recorded with the shorter wavelength and longer wavelength emission bands resemble each other and also the absorption spectrum. Thus, the two fluorescence maxima arise out of the single species of PQ- $\beta\text{-CD}$ with the same

Fig. 3 Fluorescence spectra of PQ ($1.8 \times 10^{-5} \text{ mol}\cdot\text{dm}^{-3}$) with increasing concentrations of $\beta\text{-CD}$ at pH = 6.5 (1), 0; (2), 0.002; (3), 0.004; (4), 0.006; (5), 0.008, (6), 0.010 and (7), $0.012 \text{ mol}\cdot\text{dm}^{-3}$ $\beta\text{-CD}$



ground state precursor. It also shows the absence of any red edge effect. Hence, the fluorescence intensity of PQ- β -CD complex has two fluorescence maxima.

The Benesi–Hildebrand, BH, equation (Eq. 7) for the 1:1 inclusion complex is given by

$$\frac{1}{(I - I_0)} = \frac{1}{(I' - I_0)} + \frac{1}{K(I' - I_0)[\beta\text{-CD}]} \quad (7)$$

The slope was obtained from the BH plots (Fig. 4a and b) and was used to calculate the binding constant K by Eq. 8 and is found to be 168.23 and 213.33 at 303 K.

$$K = \frac{1}{\text{slope}(I' - I_0)} \quad (8)$$

Normally the binding constant values are independent of the method. However, we observed different values in ground and excited state analysis [30]. This may result from instrumental error. The spectral influences of β -CD on the guest molecules in the excited state is more pronounced than in ground state [30] and this might be a reason for high binding constant values.

3.1.3 Gibbs Energy of Inclusion

The standard state Gibbs energy change (ΔG^0) was calculated using Eq. 9,

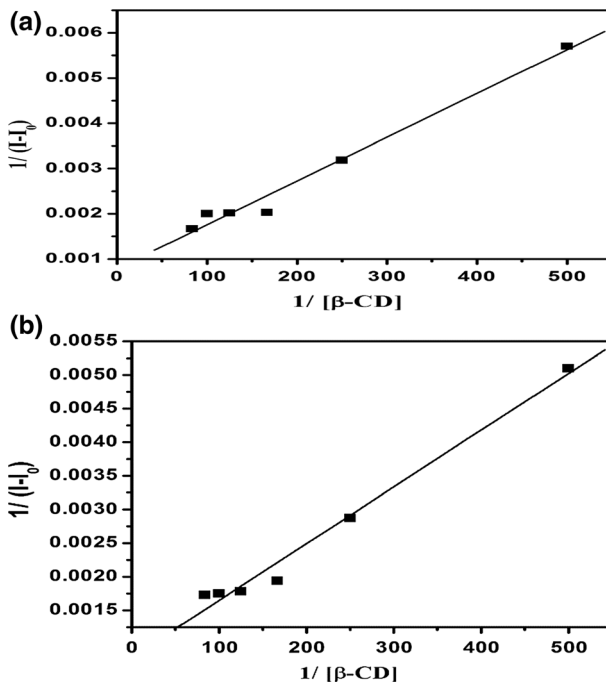


Fig. 4 **a** Benesi–Hildebrand emission plot of $1/(I - I')$ against $1/[\beta\text{-CD}]$ for PQ ($\lambda_{\text{flu}} = 359.0$ nm); **b** Benesi–Hildebrand emission plot of $1/(I - I_0)$ against $1/[\beta\text{-CD}]$ for PQ ($\lambda_{\text{flu}} = 372.0$ nm)

$$\Delta G^0 = -2.303 RT \log_{10} K \quad (9)$$

where, R is the gas constant, T is the temperature and K was the binding constant. K was obtained from the changes in absorbance and fluorescence intensities of PQ with β -CD (Table 2).

3.1.4 Lifetime

In order to get supporting evidence for the complexation of PQ with β -CD, lifetime analysis was carried out in the liquid state. Decay lifetimes of PQ with increasing concentration of β -CD are given in Fig. 5. The relevant data are given in Table 3. In aqueous medium, the PQ molecule exhibits three exponential factors with three T values (T_1 , T_2 and T_3). The lifetime and relative amplitude showed that the PQ molecule is dispersed into three states. Addition of β -CD to the PQ solution caused the relative amplitude to increase. The lifetime and amplitude of the free form remains constant and those of the complexed form are higher. An increased lifetime and relative amplitude of PQ molecule in β -CD solutions confirmed the formation of the complex. At highest concentration of β -CD, the lifetime of complexed species (T_1) and relative amplitude are 8.14×10^{-11} and 26.72%, respectively.

Table 2 Statistical parameters for the inclusion complex of PQ with β -CD

Parameters	Absorption spectra	Fluorescence spectra	
	λ_{abs} at 261.0 nm	λ_{emi} at 359.0 nm	λ_{emi} at 372.0 nm
r^2	0.9973	0.991	0.9917
Standard deviation	1.203×10^{-4}	2.29×10^{-4}	1.91×10^{-4}
Stoichiometry	1:1	1:1	1:1
K ($\text{mol}\cdot\text{dm}^{-3}$) ⁻¹	114.478	168.23	213.33
ΔG^0 ($\text{kJ}\cdot\text{mol}^{-1}$)	- 12.0	- 12.7	- 13.5

Fig. 5 Fluorescence decay curves for PQ (1.8×10^{-5} $\text{mol}\cdot\text{dm}^{-3}$) with various concentrations of β -CD ($\text{mol}\cdot\text{dm}^{-3}$): (1) without β -CD, (2) 2×10^{-3} , (3) 4×10^{-3} , (4) 6×10^{-3} , (5) 8×10^{-3} , (6) 10×10^{-3} and (7) 12×10^{-3} $\text{mol}\cdot\text{dm}^{-3}$

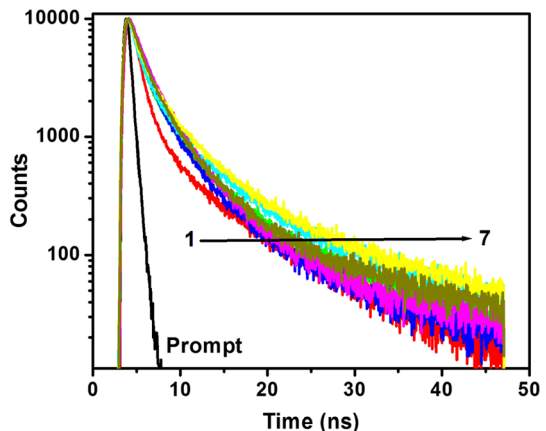


Table 3 Lifetime data of PQ with different concentrations of β -CD (excitation wavelength is 290.0 nm and emission wavelength is 360.0 nm)

$[\beta\text{-CD}]$ (mol·dm ⁻³)	Lifetime (s)	Relative amplitude	χ^2	Standard deviation
Without β -CD	5.69×10^{-11}	35.09	1.25	2.16×10^{-12}
	1.15×10^{-9}	28.80		1.74×10^{-11}
	7.55×10^{-9}	36.12		6.56×10^{-11}
2×10^{-3}	2.23×10^{-11}	57.65	1.36	2.59×10^{-11}
	1.74×10^{-9}	20.20		3.83×10^{-11}
	6.86×10^{-9}	22.15		6.26×10^{-11}
4×10^{-3}	6.39×10^{-11}	27.27	1.34	3.86×10^{-13}
	1.77×10^{-9}	38.35		2.90×10^{-11}
	6.17×10^{-9}	34.37		5.69×10^{-11}
6×10^{-3}	6.50×10^{-11}	25.36	1.34	1.00×10^{-12}
	1.71×10^{-9}	30.73		3.18×10^{-11}
	7.18×10^{-9}	43.91		5.82×10^{-11}
8×10^{-3}	5.80×10^{-11}	23.20	1.23	3.92×10^{-13}
	1.94×10^{-9}	43.73		3.32×10^{-11}
	5.89×10^{-9}	33.06		5.25×10^{-11}
10×10^{-3}	6.52×10^{-11}	22.26	1.34	8.87×10^{-13}
	1.79×10^{-9}	32.11		3.03×10^{-11}
	6.97×10^{-9}	45.64		5.36×10^{-11}
12×10^{-3}	8.14×10^{-10}	26.72	1.12	7.63×10^{-11}
	2.79×10^{-9}	53.45		6.14×10^{-11}
	9.33×10^{-9}	19.83		2.24×10^{-10}

3.2 Effect of pH

3.2.1 Effect of Proton Ion Concentration on PQ in Aqueous Medium

The absorption and fluorescence spectroscopy were used to determine the acid dissociation constants of a molecule in the absence and presence of β -CD [34] at the ground and excited singlet state by spectrophotometric and fluorimetric titration and in some cases by the Förster cycle [35].

The effect of acidity on the absorption spectra of PQ has been studied in the pH range from 1.5 to 7.5 in aqueous medium (Fig. 6). The absorption maximum of the neutral form of PQ is at 260 nm. When the pH is lowered, a blue-shifted maximum at 255.0 nm (Table 4) is obtained at around pH = 3.6. This blue-shifted maximum corresponds to the monocation obtained by protonation of the amino group. Further increase in acid concentration does not change the absorption spectrum significantly, while on increasing pH from 7.0 to 12.0 there is no remarkable change in the absorption spectrum. For the monocation–neutral equilibrium of PQ a clear isosbestic point is obtained at 254.0 nm.

The ground state pK_a value for the monocation–neutral equilibrium of PQ (Eq. 10) in aqueous medium was determined to be 3.4 spectrophotometrically (Table 6).

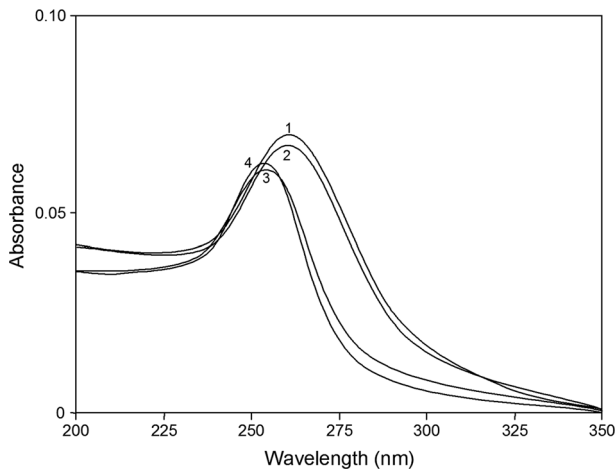


Fig. 6 Absorption spectra of PQ ($1.8 \times 10^{-5} \text{ mol} \cdot \text{dm}^{-3}$) in aqueous solution at different pH values: (1) 7.5, (2) 5.5, (3) 3.5, (4) 1.5

Table 4 Absorption and fluorescence spectral maxima of PQ in aqueous medium

Solution no.	pH	Without β -CD	
		UV (nm)	Flu (nm)
1	7.5	260.0	375.0
2	5.5	260.0	370.0
3	3.5	255.0	339.0
4	1.5	254.0	335.0



The fluorescence spectra of PQ in aqueous solutions at different pH values are shown in Fig. 7. The neutral species of PQ at pH = 7.5 shows a fluorescence maximum at 375.0 nm. When the pH is decreased, a larger blue shifted maximum is observed at 339.0 nm at pH 3.5 (Table 4). This shifted maximum is due to the monocation of PQ obtained by the protonation of the amino group. No further shifts in the maximum and its intensity are observed beyond pH = 7.5. The fluorimetric titration curve (FT curve) for the monocation–neutral equilibrium of PQ is shown in Fig. 8. The FT curve is drawn between 375.0 nm and 335.0 nm. The excited state pK_a (pK_a^*) value obtained from the inflections of these curves is found to be 3.3 (Table 6).

Based on the proton transfer ability of PQ in aqueous medium, we proposed a possible structure and relevant equilibrium for the PQ (Fig. 9). Among them, I is the preferred based on the molecular docking analysis.

3.2.2 Effect of Proton Concentration on PQ in β -CD Solutions

Figure 10 shows the UV spectra of PQ in the presence of β -CD at various pH values. The PQ absorption maximum at 262.0 nm is due to in neutral form. At pH = 3.5, the absorption

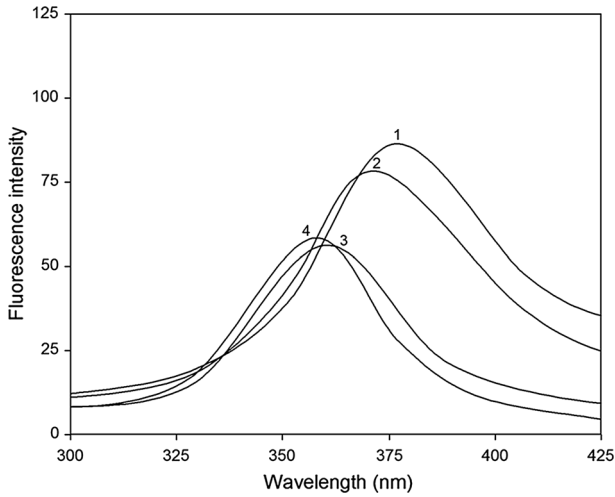


Fig. 7 Fluorescence spectra of PQ ($1.8 \times 10^{-5} \text{ mol-dm}^{-3}$) in aqueous solution at different pH values: (1) 7.5, (2) 5.5, (3) 3.5, (4) 1.5

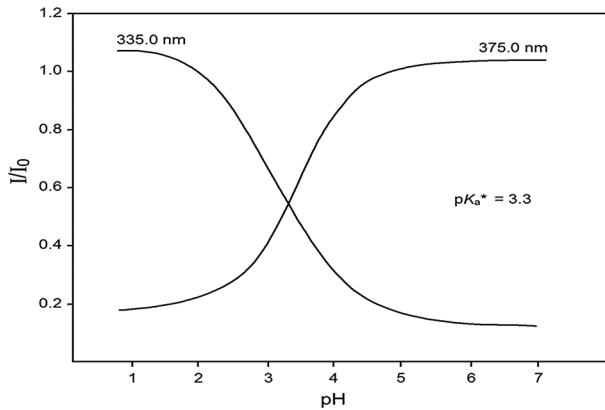
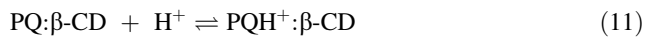


Fig. 8 FT curves of PQ in aqueous medium

maximum is slightly blue shifted (255.0 nm). The blue shifted maximum (Table 5) is due to the protonation of the amino group of the PQ molecule encapsulated in the β -CD cavity. Even at pH = 1.5, the spectral maximum remains unchanged. Hence, protonation of the amino group is completed at pH = 3.5. The ground state acidity constant (pK_a) value was calculated for the equilibrium between neutral and monocation of PQ in β -CD medium (Eq. 11) and the value is 3.4.



The fluorescence spectra of PQ in β -CD solutions with different pH values are shown in Fig. 11. Initially, at pH = 7.5, the PQ molecule showed two emission maxima at 361.00 and 371.0 nm. The two emission maxima are observed for PQ in its neutral form at neutral pH

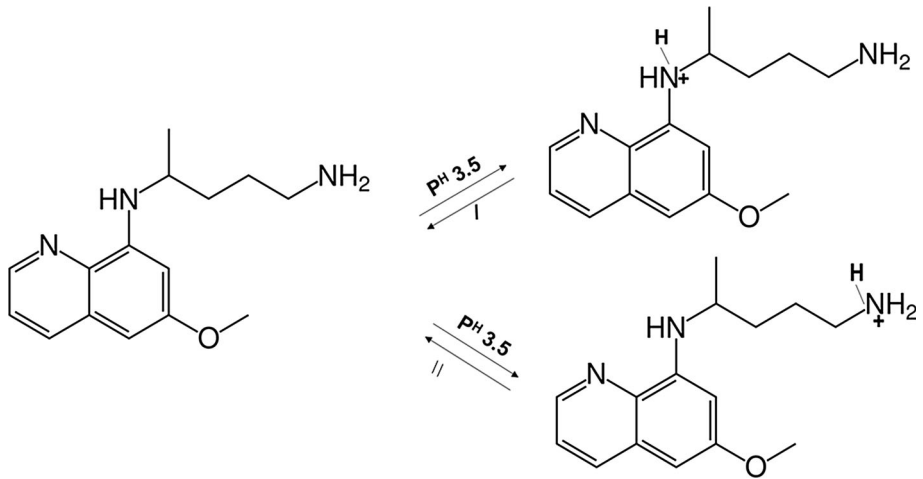


Fig. 9 Equilibrium between the neutral and monocation of PQ in aqueous medium

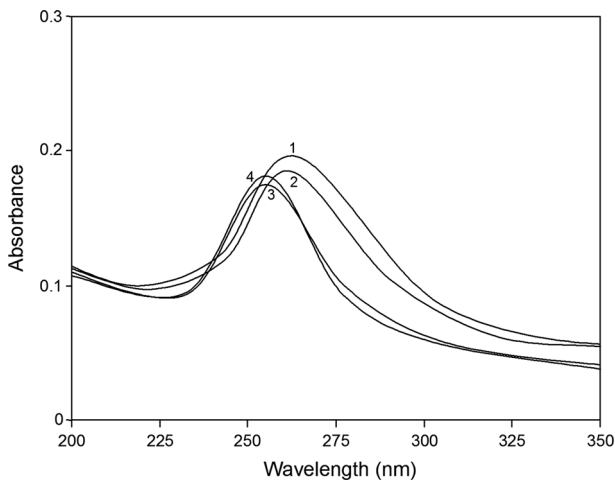


Fig. 10 Absorption spectra of PQ ($1.8 \times 10^{-5} \text{ mol}\cdot\text{dm}^{-3}$) in β -CD ($0.012 \text{ mol}\cdot\text{dm}^{-3}$) solutions at different pH values: (1) 7.5, (2) 5.5, (3) 3.5, (4) 1.5

Table 5 Absorption and fluorescence spectral maxima of PQ in β -CD medium

Solution no.	pH	With β -CD		
		UV (nm)	Flu (nm)	Flu (nm)
1	7.5	262.0	361.0	371.0
2	5.5	261.5	360.0	371.0
3	3.5	255.0	352.0	–
4	1.5	255.0	352.0	–

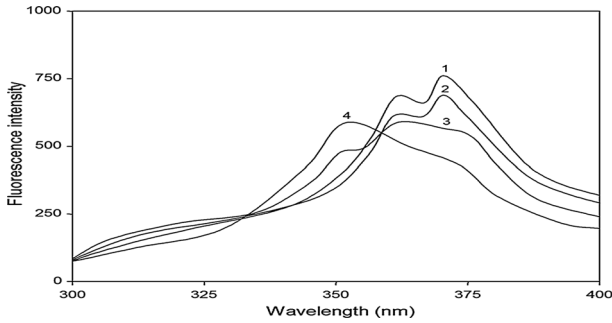


Fig. 11 Fluorescence spectra of PQ (1.8×10^{-5} mol·dm $^{-3}$) in β -CD (0.012 mol·dm $^{-3}$) solution at different pH values: (1) 7.5, (2) 5.5, (3) 3.5, (4) 1.5

levels. The two emission maxima are retained to pH = 5.5. Below pH = 5.5, the emission maximum appeared at 350 nm (Table 5) indicating the formation of the monocation by protonation at the amino group of PQ. The FT curve was drawn to find the excited state acidity constant (pK_a^*) for the monocation \rightleftharpoons neutral equilibrium of the PQ molecule in β -CD media. The two curves (λ_{flu} at 370.0 and 355.0 nm) are met at 3.5 (Table 6) and it represented as pK_a^* for the PQ molecule in the β -CD cavity (Fig. 12).

The ground and excited state acidity constants (pK_a and pK_a^*) for the monocation–neutral equilibrium of PQ, in the absence and presence of β -CD, are given in Table 6. This indicates the $-NH$ group of PQ lies outside the cavity of β -CD.

Table 6 pK_a and pK_a^* values of PQ in aqueous and β -CD media

Solution no.	Medium	Acidity constant	
		pK_a	pK_a^*
1	PQ without β -CD	3.4	3.3
2	PQ with β -CD	3.4	3.3

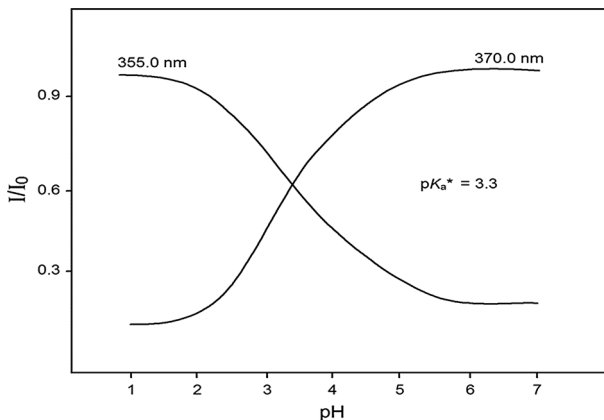


Fig. 12 FT curves of PQ in β -CD medium

Based on the proton ion transfer ability of PQ in β -CD medium, we proposed a possible structure and relevant equilibrium for the PQ: β -CD (Fig. 13). Among them, I is the more preferable one based on the molecular docking analysis.

3.3 Interaction of PQ with β -CD in Solid State

3.3.1 FT-IR Spectral Analysis

The FT-IR technique is one of the most important and powerful techniques for the confirmation of the inclusion complex between PQ and β -CD in the solid state. FT-IR spectra of pure β -CD and PQ and the CP, PM and KM products are shown in the Fig. 14 and the relevant data are given in the Table 7. Among all the stretching and bending vibrations, we have chosen some selective frequencies for the discussion. The stretching frequencies for the aromatic N–H, aromatic C=C, aromatic C–H and aromatic C–N of pure PQ appear at 1333.93, 2966.68, 2948.58 and 1265.29 cm^{-1} , respectively. These frequencies are significantly changed to 1337.99, 2970.85, 2929.28 and 1295.44 cm^{-1} , respectively for the CP products with the above stretching vibrations. Further, the stretching frequencies for aromatic C–C, aliphatic C–H and aliphatic C–N of PQ appear at 1469.67, 2879.68 and 1194.15 cm^{-1} , respectively, and are remarkably shifted to 1459.59, 2875.00 and 1200.93 cm^{-1} for the CP product. Thus, the changes in the stretching frequencies may be taken as the confirmation for the inclusion complex between PQ with β -CD. Notably, there are no significant changes in all the stretching frequencies for the PM and KM products.

3.3.2 Powder X-ray Diffraction Analysis

XRD is a rapid analytical technique and it is the primarily used for the determination of crystalline nature of a compound. The diffractogram of pure PQ and β -CD and of the PM, KM, and CP products are shown in the Fig. 15. By comparing the diffractogram of pure PQ with products, we can get some idea about the formation of inclusion complexes between

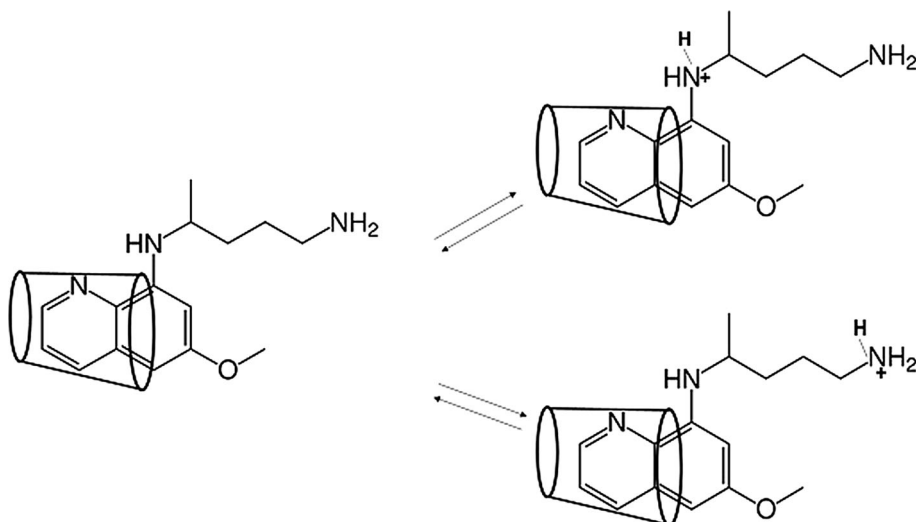


Fig. 13 Equilibrium between the neutral and monocation of PQ in β -CD medium

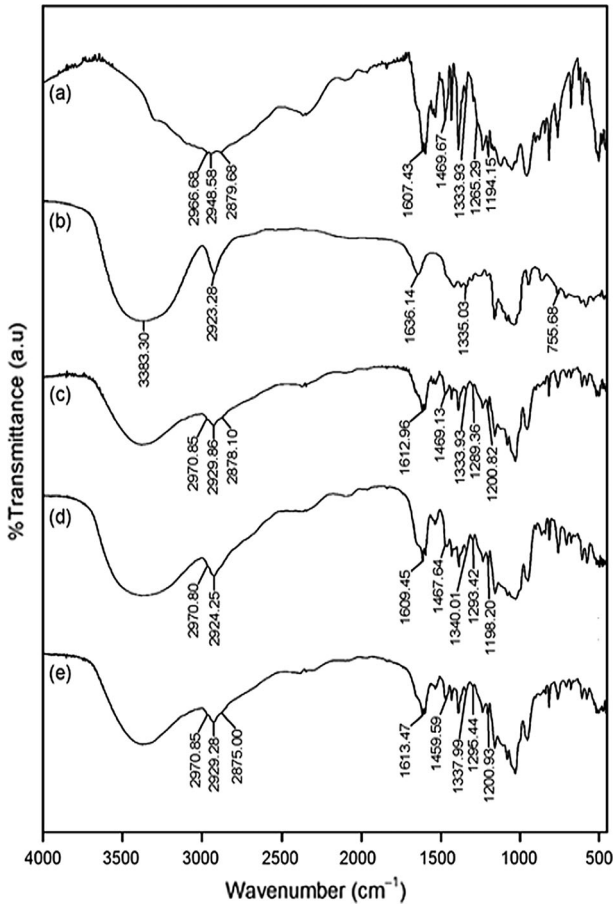


Fig. 14 FT-IR spectra of (a) PQ, (b) β -CD, (c) physical mixture, (d) kneaded mixture and (e) coprecipitated products

Table 7 FT-IR Stretching frequencies of pure PQ and the PM, KM and CP products

Sample	Stretching frequency	PQ (cm^{-1})	PM (cm^{-1})	KM (cm^{-1})	CP (cm^{-1})
1	Aliphatic primary amine	1607.43	1612.96	1609.45	1613.47
2	Aromatic tertiary amine	1333.93	1333.93	1340.01	1337.99
3	Aromatic C=C	2966.68	2970.85	2970.80	2970.85
4	Aromatic C–H	2948.58	2929.86	2924.25	2929.28
5	Aromatic C–N	1265.29	1289.36	1293.42	1295.44
6	Aromatic C–C	1469.67	1469.13	1467.64	1459.59
7	Aliphatic CH group	2879.68	2878.10	Disappeared	2875.00
8	Aliphatic C–N	1194.15	1200.82	1198.20	1200.93

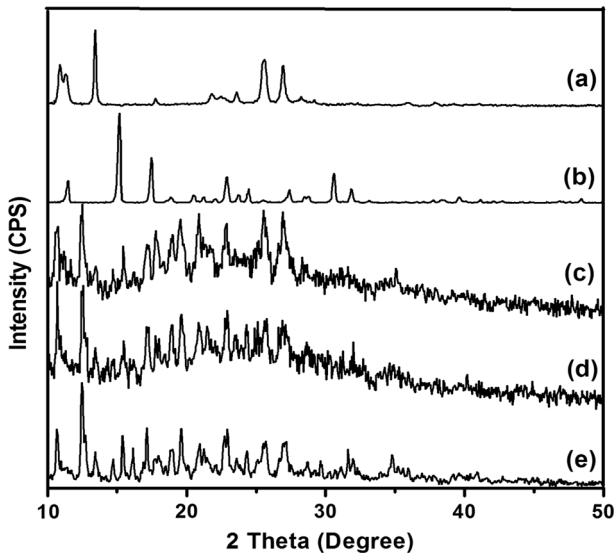


Fig. 15 Powder XRD patterns of (a) PQ, (b) β -CD, (c) physical mixture, (d) kneaded mixture and (e) coprecipitated products

β -CD and PQ. Pure PQ shows some important peaks at the diffraction angle of 2θ at 10.87° , 11.27° , 12.37° , 17.72° and 21.77° . These diffraction peaks are not observed in the solid products obtained by the PM, KM and CP methods. The CP product shows diffraction angles of 2θ at 10.67° , 11.32° , 12.47° , 17.97° and 21.22° . At the same time, the PM and KM products show some minor changes in the XRD patterns. In our view, these do not coincide with CP products completely and the CP is little influenced by β -CD in these products.

3.3.3 SEM Image Analysis

Scanning electron microscopy is mainly used for observing modifications of surface morphology. SEM images of pure PQ and β -CD and of the PM, KM and CP products are shown in the Fig. 16. The SEM image of β -CD shows clear rock like structures [30] and PQ showed needle like structures. The morphology of the CP product is completely different from either of these. As the morphology of the CP product is different, it can be taken as secondary evidence for complex formation. On the other hand, the PM and KM products show morphologies resembling physical mixtures with of PQ and β -CD, showing that the two compounds have not reacted with each other. Thus, no complex formation is observed in the PM and KM products.

3.3.4 Differential Scanning Colorimetry

DSC analysis is a simple and reliable technique used for the preliminary investigation of thermal behavior for the compound and their inclusion complexes obtained by the standard procedure. Generally, when the guest molecule is included into the β -CD cavity, their

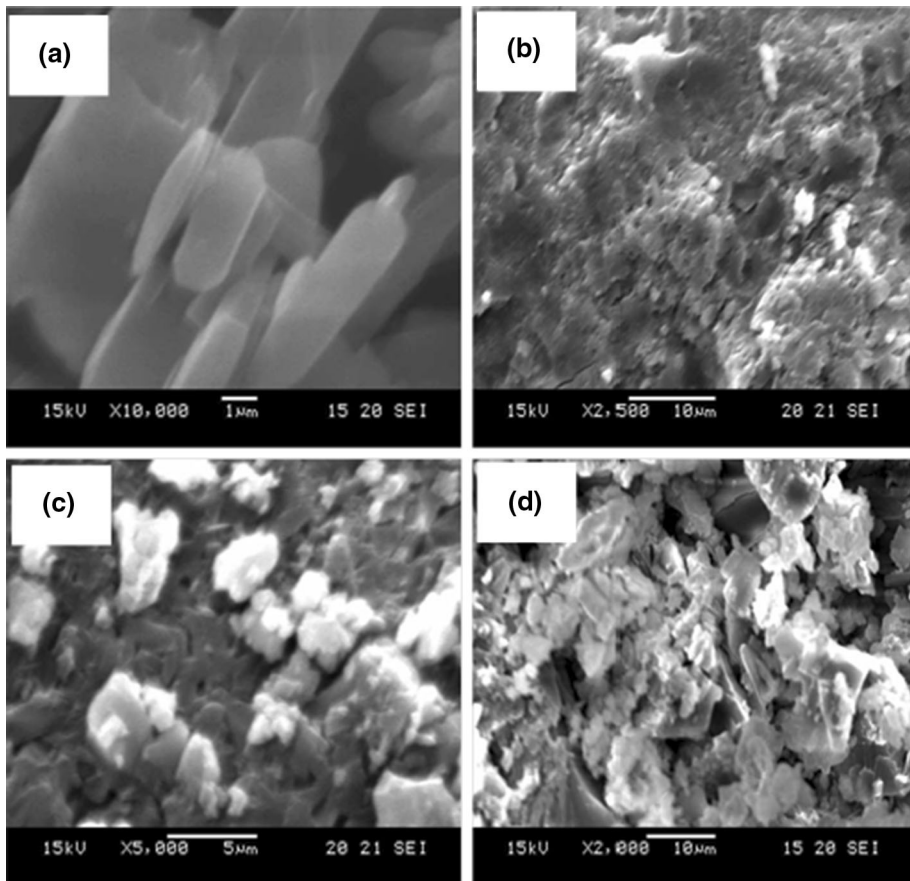


Fig. 16 SEM images of **a** PQ, **b** physical mixture, **c** kneaded mixture and **d** coprecipitated products

melting point, sublimation point and boiling point may be shifted to different temperatures or sometimes disappear.

The DSC traces for pure PQ and β -CD and of the PM, KM and CP products are shown in Fig. 17. The measured melting point of PQ is 200.13 °C while those of the CP, KM and PM products are 195.4, 200.49 and 198.9 °C, respectively. The melting point of the CP product is lower than that of the pure PQ, consistent with an interaction between the PQ and β -CD molecules. Those of the KM and PM products are much less changed than the CP product.

3.3.5 Molecular Docking Study of the Inclusion Complex

The three dimensional structure of β -CD and PQ were obtained from crystallographic databases and are shown in Fig. 18a and b. The guest molecule, PQ was docked into the cavity of β -CD using the Patch-Dock server. Based on the energetic parameters, including

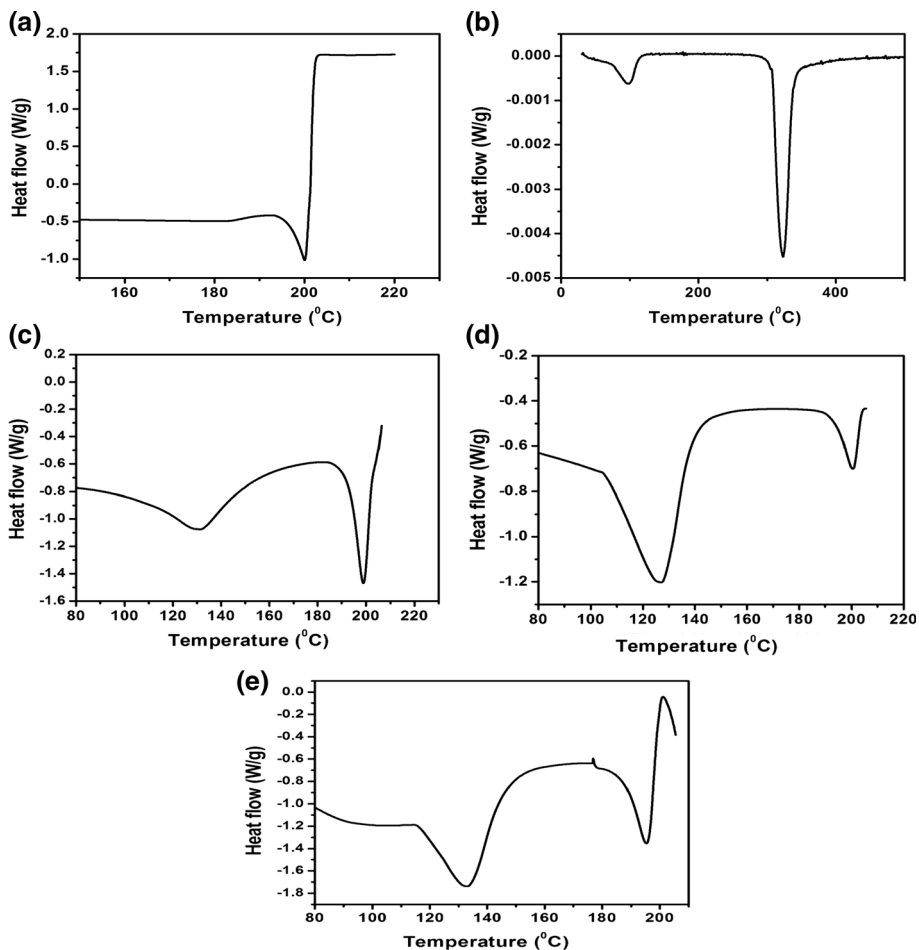


Fig. 17 DSC patterns of **a** PQ, **b** β -CD, **c** physical mixture, **d** kneaded mixture and **e** coprecipitated products

the geometric shape complementarity score [36], approximate interface area size and atomic contact energy [29] of the PQ: β -CD inclusion complex, the Patch-Dock server provided several possible docked models for the most probable structure (Table 8). The docked PQ: β -CD 1:1 model (Fig. 18c) with the highest geometric shape complementarity score (3730), approximate interface area size of the complex (477 \AA^2) and lowest atomic contact energy ($-1262.6 \text{ kJ}\cdot\text{mol}^{-1}$) was the most probable and energetically favorable model.

3.3.6 Semi-Empirical Quantum Mechanical Calculations

The internal diameter of the β -CD is approximately 6.5 \AA and its height is 7.8 \AA as shown in Fig. 19. Considering the shape and dimensions of β -CD, it is clear that the PQ molecule cannot be completely accommodated in the β -CD cavity, because, the overall height of PQ

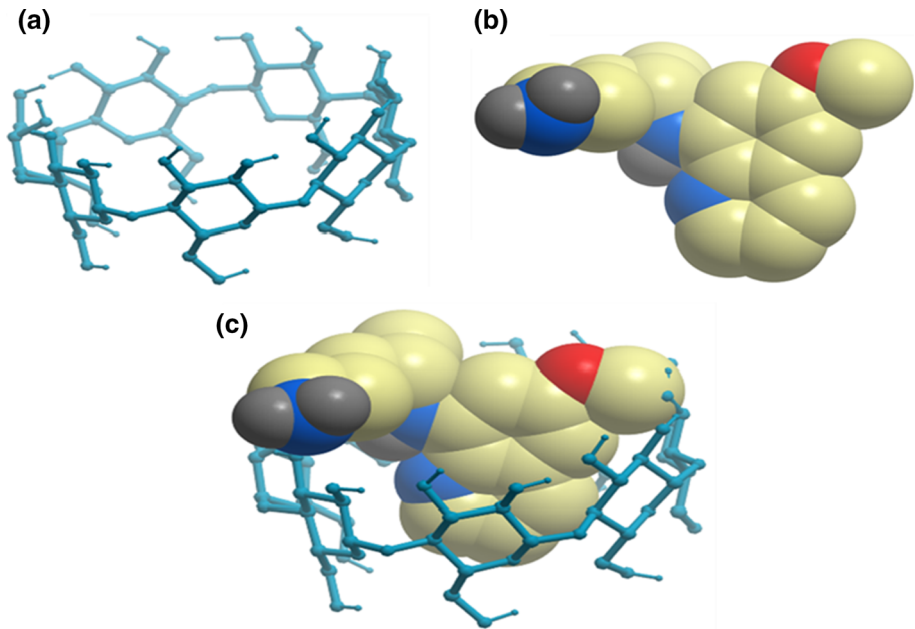


Fig. 18 Ball and stick representation of **a** β -CD, **b** PQ, **c** PQ and β -CD 1:1 inclusion complex; the hydroxyl group is shown as red, nitrogen as blue, carbon as golden, chloride as green and hydrogen atoms are not shown

Table 8 Scores of the top 10 docked models of PQ: β -CD inclusion complex computed using the Patch-Dock server

Model	Geometric shape complementarity score	Approximate interface area size of the complex (\AA^2)	Atomic contact energy ($\text{kJ}\cdot\text{mol}^{-1}$)
1	3730	477.00	-1262.6
2	3616	433.80	-1230.2
3	3554	428.40	-1197.9
4	3548	461.40	-1260.1
5	3522	469.10	-969.9
6	3518	421.70	-1203.0
7	3494	471.60	-1260.5
8	3454	390.90	-1105.5
9	3434	423.60	-1274.4
10	3432	420.20	-1230.1

is 9.40 \AA (i.e., the vertical distance between H_{30} and H_{39}), and the horizontal distance between H_{21} and H_{37} is 11.6 \AA , the internal diameter of β -CD is 6.5 \AA . Hence, it is possible to locate the PQ molecule inside the β -CD cavity as interpreted from the experimental data.

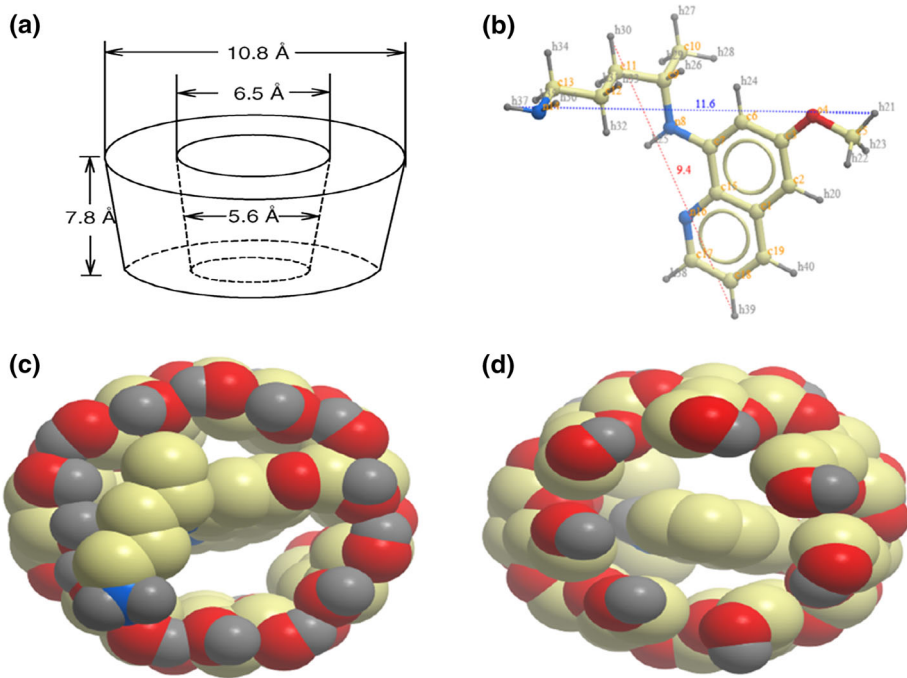


Fig. 19 Schematic diagram of **a** β-CD, **b** PQ, **c** 1:1 inclusion complex (front view), **d** 1:1 inclusion complex (back view)

3.3.7 In-vitro Anticancer Effect

Tests of the anticancer effect of PQ and its solid inclusion complexes were performed with the MDA MB 231 cell line (Table 9). Solutions of PQ and the solid inclusion complex were prepared with concentrations: 62.5, 125, 250, 500 and 1000 mg·mL⁻¹.

Table 9 In-vitro cytotoxic activity of PQ and its solid complex with CD on the MDA MB 231 cell line

Sample	Name of the samples	Conc. (μg·mL ⁻¹)	% of cytotoxicity	CTC ₅₀ (μg·mL ⁻¹)
1	PQ	1000	89.63±0.7	68.33±2.9
		500	89.12±0.4	
		250	87.97±1.9	
		125	84.65±0.7	
		62.5	47.19±0.7	
2	PQ solid complex	1000	89.84±0.3	123.33±2.9
		500	88.90±0.3	
		250	84.99±0.4	
		125	51.19±1.6	
		62.5	35.59±3.6	

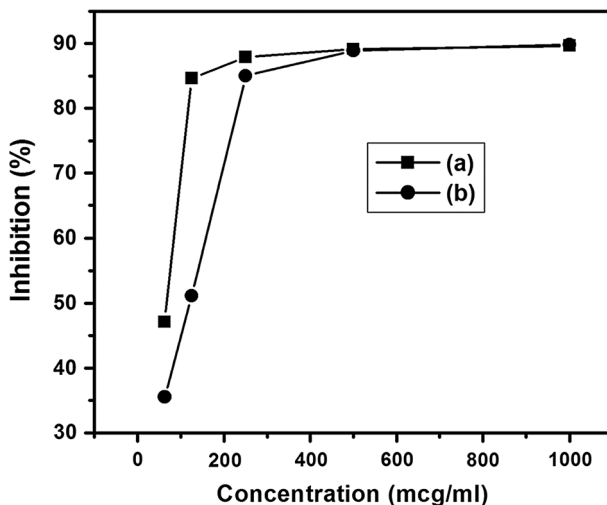


Fig. 20 Percentage of inhibition of (1) pure PQ, (2) solid complex on MDA MB 231 cell line

The percentages of inhibition increase with increasing concentration of pure PQ and the solid inclusion complexes are shown in Fig. 20; the related photographs are presented in Fig. 21. CP was not found to have better results than PQ alone; however, the activity is slightly higher at the higher concentration of the solid complex ($1000 \text{ mg}\cdot\text{mL}^{-1}$) than that of pure PQ. Thus, pure PQ showed the better anticancer activity than the CP product at lower concentration but the activities are marginally reversed at the higher concentration.

4 Conclusions

In this paper, an inclusion complex of PQ: β -CD with 1:1 stoichiometric ratio was prepared by physical, kneading and co-precipitation methods. The inclusion interaction of PQ with β -CD was analyzed by UV and fluorescence spectroscopy in the liquid state. Two emission maxima are observed for PQ in both water and β -CD solutions. Lifetime and relative amplitudes of these are highly increased by the addition of β -CD. The complexing ability of PQ with β -CD in the solid state was further analyzed by FT-IR, powder XRD, DSC and SEM. These suggest that PQ is encapsulated with the cavity of β -CD. The energetically more favorable inclusion complex is obtained by molecular docking studies. Both the experimental and molecular docking methods showed that the PQ is included in the β -CD cavity. No substantial changes are obtained in the anti-cancer activity for both PQ and its CP products against the breast cancer cell line at the lower concentrations.

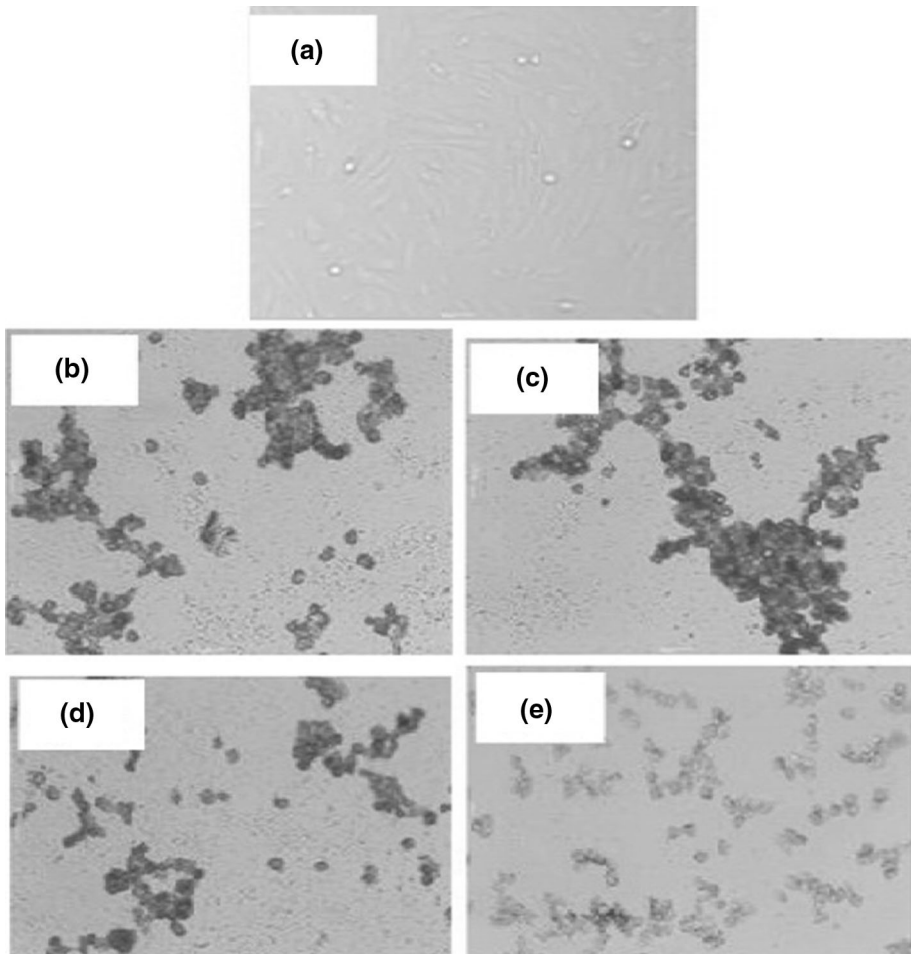


Fig. 21 Photos of **a** MDA MB 231 Control, **b** PQ Pure-1000C, **c** PQ Pure-500C, **d** solid Complex-1000C, **e** Solid Complex-500C

References

1. Baird, K., Stephen, J., Hoffman, L.: Primaquine therapy for malaria. *Clin. Infect. Dis.* **39**, 1336–1345 (2014)
2. Freudenberg, K., Cramer, F., Plieninger, H.: Inclusion Compounds of Physiologically Active Organic Compounds. German Pat. 895769 (1953)
3. Szejtli, J., Szente, L.: Elimination of bitter, disgusting tastes of drugs and foods by cyclodextrins. *Eur. J. Pharm. Biopharm.* **61**, 115–125 (2005)
4. Shityakov, S., Broscheit, J., Förster, C.: α -Cyclodextrin dimer complexes of dopamine and levodopa derivatives to assess drug delivery to the central nervous system: ADME and molecular docking studies. *Int. J. Nanomed.* **7**, 3211–3219 (2012)
5. Lee, C.W., Kim, S.J., Youn, Y.S., Widjojokusumo, E., Lee, Y.H., Kim, J., Lee, Y.W., Tjandrawinata, R. R.: Preparation of bitter taste masked cetirizine dihydrochloride/ β -cyclodextrin inclusion complex by supercritical anti-solvent (SAS) process. *J. Supercrit. Flu.* **55**, 348–357 (2010)

6. Charlton, A.J., Davis, A.L., Jones, D.P., Lewis, J.R., Davies, A.P., Haslam, E., Williamson, M.P.: The self-association of the black tea polyphenol theaflavin and its complexation with caffeine. *J. Chem. Soc. Perkin Trans. 2*, 317–322 (2000)
7. Al-Maaieh, A., Flanagan, D.R.: Salt effects on caffeine solubility, distribution, and self-association. *J. Pharm. Sci.* **91**, 1000–1008 (2001)
8. Poltev, V.I., Grokhlina, T.I., González, A., Deriabina, Q., Cruz, L., Gor, J., Leszczynski, L.N., Djimant, A.N.: Veselkov.: the study of three-dimensional structure of caffeine associates using computational and experimental methods. *J. Mol. Struct.* **709**, 123–128 (2004)
9. Dong, Z., Liang, Y.R., Fan, F.Y., Ye, J.H., Zheng, X.Q., Lu, J.L.: Adsorption behavior of the catechins and caffeine onto polyvinylpyrrolidone. *J. Agric. Food Chem.* **59**, 4238–4247 (2011)
10. Murugan, M., Rajamohan, R., Sivakumar, K.: A study of host-guest complexation between amodiaquine and native cyclodextrin. Characterization in solid state and its in vitro anticancer activity. *J. Macromol. Sci. A* **53**, 282–283 (2016)
11. Anitha, A., Murugan, M., Rajamohan, R.: Molecular encapsulation of amodiaquine in 2-hydroxypropyl β -cyclodextrin cavity. *Spectros. Lett.* (2018). <https://doi.org/10.1080/003877010.2018.1448421>
12. Bhardwaj, R., Dorr, R.T., Blanchard, J.: Approaches to reducing toxicity of parenteral anticancer drug formulations using cyclodextrins. *J. Pharm. Sci. Technol.* **54**, 233–239 (2000)
13. Fujishima, N., Kusaka, K., Umino, T., Urushinata, T., Terumi, K.: Flour based foods containing highly branched cyclodextrins. *Jpn. Patent JP* **136**, 898 (2001)
14. Holland, L., Rizzi, G., Malton, P.: Cosmetic compositions comprising cyclic oligosaccharides and fragrance. *PCT Int. Appl.* **67**, 716 (1999)
15. Lezcano, M., Ai-Soufi, W., Novo, M., Rodriguez-Nunez, E., Tato, J.V.: Complexation of several benzimidazole-type fungicides with alpha and beta cyclodextrins. *J. Agric. Food Chem.* **50**, 108–112 (2002)
16. Dufosse, J., Souchon, I., Feron, G., Latrasse, A., Spinnler, H.E.: In situ detoxification of the fermentation medium during γ -decalactone production with the yeast *Sporidiobolus salmonicolor*. *Biotech. Prog.* **15**, 135–139 (1999)
17. Zhou, J., Ritter, H.: Cyclodextrin functionalized polymers as drug delivery systems. *Pol. Chem.* **1**, 1552–1559 (2010)
18. Hedges, R.A.: Industrial applications of cyclodextrins. *Chem. Rev.* **98**, 2035–2044 (1998)
19. Zhang, X., Wang, C.: Supramolecular amphiphiles. *Chem. Soc. Rev.* **40**, 94–101 (2011)
20. Harada, A., Takashima, Y., Yamaguchi, H.: Cyclodextrin-based supramolecular polymers. *Chem. Soc. Rev.* **38**, 875–882 (2009)
21. Chen, Y., Liu, Y.: Cyclodextrin-based bioactive supramolecular assemblies. *Chem. Soc. Rev.* **39**, 495–505 (2010)
22. Nakahata, M., Takashima, Y., Yamaguchi, H., Harada, A.: Redox-responsive self-healing materials formed from host–guest polymers. *Nat. Commun.* **2**, 511 (2011)
23. Chen, G., Jiang, M.: Cyclodextrin-based inclusion complexation bridging supramolecular chemistry and macromolecular self-assembly. *Chem. Soc. Rev.* **40**, 2254–2266 (2011)
24. Hetzer, M., Schmidt, B.V.K.J., Barner-Kowollik, C., Ritter, H.: Limitations of cyclodextrin-mediated RAFT homo polymerization and block copolymer formation. *J. Pol. Sci. Part A.* **51**, 2504–2517 (2013)
25. Schmidt, B.V.K.J., Hetzer, M., Ritter, H., Barner-Kowollik, C.: Cyclodextrin-complexed RAFT agents for the ambient temperature aqueous living/controlled radical polymerization of acrylamido monomers. *Macromolecules* **44**, 7220–7232 (2011)
26. Schneidman-Duhovny, D., Inbar, Y., Nussinov, R., Wolfson, H.J.: PatchDock and Symm Dock: servers for rigid and symmetric docking. *Nucl. Acids Res.* **33**, 363–367 (2005)
27. Connolly, M.L.: Solvent-accessible surfaces of proteins and nucleic acids. *Science* **221**, 709–711 (1983)
28. Connolly, M.L.: Analytical molecular surface calculation. *J. Appl. Crystallogr.* **16**, 548–558 (1983)
29. Zhang, C., Vasmatzis, G., Cornette, J.L., DeLisi, C.: Determination of atomic desolvation energies from the structures of crystallized proteins. *J. Mol. Biol.* **267**, 707–726 (1997)
30. Prabu, S., Sivakumar, K., Swaminathan, M., Rajamohan, R.: Preparation and characterization of host–guest system between inosine and beta-cyclodextrin through inclusion mode. *Spectrochim. Acta A* **147**, 151–157 (2015)
31. Schulman, S.G., Irene, P.: Dissociation constant of the 9-anthracic acidium cation in the lowest excited singlet state. *J. Phys. Chem.* **76**, 1996–1999 (1972)
32. Misiuk, W.: Spectrofluorimetric study on inclusion interaction of beta-cyclodextrin with duloxetine and its analytical application. *I. J. Chem. Sec A.* **51**, 1706–1710 (2012)
33. Rajamohan, R., Kothai Nayaki, S., Swaminathan, M.: Investigation on association behavior between 1-aminoisoquinoline and β -cyclodextrin in solution and solid state. *J. Mol. Liq.* **220**, 918–925 (2016)

34. Enoch, M.V., Rajamohan, R., Swaminathan, M.: Fluorimetric and prototropic studies on the inclusion complexation of 3,3-diaminodiphenylsulphone with β -cyclodextrin and its unusual behavior. *Spectrochim. Acta Part A* **77**, 473–474 (2010)
35. Farag, M.A., Altalba, W.Y., Sayed, E.L., Sherbini, A.L.: Spectrophotometric determination of acidity constant of 1-methyl-4-[4'-aminostyryl]quinolinium iodide in aqueous buffer and micellar solutions in the ground and excited states. *Asian J. Chem.* **25**, 6181–6185 (2013)
36. Duhovny, D., Nussinov, R., Wolfson, H.J.: Efficient unbound docking of rigid molecules. In: Guigó, R., Gusfield, D. (eds.) *Algorithms in Bioinformatics. WABI 2002. Lecture Notes in Computer Science.* Springer, Berlin (2002)